Received: 12 September 2017 | Revised: 15 December 2017 | Accepted: 22 December 2017

DOI: 10.1111/cmi.12821

RESEARCH ARTICLE

WILEY

A male gametocyte osmiophilic body and microgamete surface protein of the rodent malaria parasite *Plasmodium yoelii* (PyMiGS) plays a critical role in male osmiophilic body formation and exflagellation

Mayumi Tachibana[1] | Tomoko Ishino[1] | Eizo Takashima[2] | Takafumi Tsuboi[2] | Motomi Torii[1]

[1] Division of Molecular Parasitology, Proteo-Science Center, Ehime University, Toon, Ehime, Japan

[2] Division of Malaria Research, Proteo-Science Center, Ehime University, Matsuyama, Ehime, Japan

Correspondence
Tomoko Ishino, Division of Molecular Parasitology, Proteo-Science Center, Ehime University, Toon, Ehime, Japan.
Email: tishino@m.ehime-u.ac.jp

Funding information
JSPS KAKENHI, Grant/Award Numbers: JP15K08443, JP24590506 and JP25670202

Abstract

Anopheles mosquitoes transmit *Plasmodium* parasites of mammals, including the species that cause malaria in humans. Malaria pathology is caused by rapid multiplication of parasites in asexual intraerythrocytic cycles. Sexual stage parasites are also produced during the intraerythrocytic cycle and are ingested by the mosquito, initiating gametogenesis and subsequent sporogonic stage development. Here, we present a *Plasmodium* protein, termed microgamete surface protein (MiGS), which has an important role in male gametocyte osmiophilic body (MOB) formation and microgamete function. MiGS is expressed exclusively in male gametocytes and microgametes, in which MiGS localises to the MOB and microgamete surface. Targeted gene disruption of MiGS in a rodent malaria parasite *Plasmodium yoelii* 17XNL generated knockout parasites (ΔPyMiGS) that proliferate normally in erythrocytes and form male and female gametocytes. The number of MOB in male gametocyte cytoplasm is markedly reduced and the exflagellation of microgametes is impaired in ΔPyMiGS. In addition, anti-PyMiGS antibody severely blocked the parasite development in the *Anopheles stephensi* mosquito. MiGS might thus be a potential novel transmission-blocking vaccine target candidate.

KEYWORDS

male gametocyte, microgamete, osmiophilic body, *Plasmodium*, transmission-blocking vaccine

1 | INTRODUCTION

Malaria is a global health problem caused by *Plasmodium* parasites, which are transmitted by *Anopheles* mosquitoes. In recent years, it has been reported that global morbidity and mortality have been reduced by using interventions such as artemisinin-based combination therapies, long-lasting insecticidal nets, and indoor residual spraying. Nevertheless, currently 212 million cases are estimated each year, resulting in 429,000 deaths annually (WHO World Malaria Report, 2016). Malaria symptoms are caused by the repeated invasion and egress of host red blood cells (RBC) by *Plasmodium* parasites. During a replication cycle, which is completed in 24–72 hr depending on the *Plasmodium* species, the merozoite invades a RBC, encapsulated by a parasitophorous vacuole membrane (PVM), where it multiplies into 10–30 new merozoites that egress from the RBC (Bannister, Hopkins, Fowler, Krishna, & Mitchell, 2000). During such cycles, some of the parasites differentiate into nonreplicative sexual stages, the gametocytes, which circulate in the blood flow until they are ingested by *Anopheles* mosquitoes. In the mosquito midgut, activated gametocytes rapidly egress from RBC and transform into gametes (Sinden, Canning, & Spain, 1976). After fertilisation and sporogonic development in the mosquito, sporozoites in the mosquito salivary glands are transmitted to a new mammalian host during a blood meal (Sinden, 1984).

To establish an infection in the mosquito, male and female gametocytes must first egress from the RBC and differentiate into mature gametes, followed by fertilisation and zygote formation. Gametogenesis is initiated by sensing mosquito midgut environmental cues, such as a drop in temperature and the presence of xanthurenic acid (Billker, Miller, & Sinden, 2000). The egress of gametocytes from RBC requires the rupture of two membranes surrounding the parasite: the inner PVM and the outer RBC membrane. The sequential inside-out lysis of PVM and RBC membrane occurs in response to the exocytosis of specialised secretory vesicles, including a subject of this study, osmiophilic bodies (OB; Sologub et al., 2011). Proteins including G377, MDV1/PEG3 (male development-1/protein of early gametocyte 3), GEST (gamete egress and sprozoite traversal), PPLP2 (plasmodial perforin-like protein 2), and MTRAP (merozoite-specific thrombospondin-related anonymous protein) were reported to be involved in this process. G377, MDV1/PEG3, and GEST are localised to the OB (Olivieri et al., 2015; Ponzi et al., 2009; Talman et al., 2011). The four proteins MDV1/PEG3, GEST, PPLP2, and MTRAP are important for efficient gametocyte egress, but G377 is not strictly essential. G377 localises to the OB of female gametocytes (Alano et al., 1995; Olivieri et al., 2015), and a dramatic decrease in the number or size of OB and delay of egress from PVM were observed in *G377* knockout female gametocytes (de Koning-Ward et al., 2008; Olivieri et al., 2015). MDV1/PEG3 is expressed in females and to a lesser degree in males and localises to the OB and parasitophorous vacuole (PV; Furuya et al., 2005). MDV1/PEG3-deficient mutants had few or no OB and were defective in PVM rupture, which leads to low transmission to mosquitoes (Ponzi et al., 2009). GEST is expressed in both male and female gametocytes and localises to the OB. GEST deficient gametocytes are not able to lyse the PVM and fail to egress from the RBC (Suaréz-Cortés et al., 2016; Talman et al., 2011). PPLP2 and MTRAP have been suggested to inhabit a separate population of egress vesicles in gametocytes. PPLP2 permeabilises RBC membrane during egress of gametocytes. PPLP2-deficient gametocytes could normally disrupt the PVM but fail to rupture the RBC membrane. The PPLP2-deficient mutant also displayed abnormal exflagellation and produced gametes with only one, shared thicker flagellum (Deligianni et al., 2013; Wirth et al., 2014). MTRAP is necessary for the disruption of the gamete-containing PVM and thus MTRAP-deficient mutants failed to egress from RBC (Bargieri et al., 2016; Kehrer, Frischknecht, & Mair, 2016). These findings provide evidence that OB and secretory vesicles play a central role in gametocyte egress from the infected RBC (iRBC). After egress from RBC, the formation of the motile flagellated microgamete occurs in a process called exflagellation and then fertilisation takes place following recognition of a macrogamete. HAP2/GCS1 (Hapless 2/Generative Cell Specific 1), a homologue of a sterility gene in both *Arabidopsis* and green alga *Chlamydomonas*, is expressed in male gametocytes and microgametes and has an important role in the fertilisation process. HAP2/GCS1 is essential for gamete fusion in *Plasmodium* (Blagborough & Sinden, 2009; Liu et al., 2008).

Here, we report that one of the putative egress related proteins, *Plasmodium yoelii* microgamete surface protein (PyMiGS), described as an aspartyl protease (Kehrer et al., 2016), is specifically expressed in male gametocytes and microgametes and is localised to the gametocyte MOB and surface of microgametes. PyMiGS is important for male gametocyte MOB formation but is dispensable for male gametocyte egress from RBC. Decreased exflagellation efficiency and zygote/ookinete formation of PyMiGS-deficient parasite suggests that PyMiGS partially contributes to the male gamete exflagellation process. Because PyMiGS is localised to the microgamete surface, we examined the possibility that this molecule might serve as a transmission-blocking vaccine (TBV) target. Antibody against PyMiGS dramatically reduced the formation of oocysts on the mosquito midgut. These results indicate that PyMiGS could be a novel malaria TBV candidate.

2 | RESULTS

2.1 | PyMiGS is expressed in male gametocytes and microgametes

PyMiGS (PY17X_1451500) is a 594 amino acid protein containing an N-terminal signal peptide, aspartyl protease-like domain, and a C-terminal transmembrane domain (Figure S1a). The aspartyl protease-like domain is conserved among MiGS orthologues in other *Plasmodium* species (http://www.plasmodb.org).

To characterise the expression and localisation of PyMiGS, we raised rabbit antibody against nearly full-length recombinant PyMiGS protein, which lacks the N-terminal signal peptide and C-terminal transmembrane domain, expressed by the wheat germ cell-free protein synthesis system (WGCFS; Figure S1a; Tsuboi, Takeo, et al., 2008; Tsuboi, Takeo, Sawasaki, Torii, & Endo, 2010). To evaluate the reactivity of the antiserum against parasite-derived PyMiGS, western blotting analysis was performed using gametocyte-enriched *P. yoelii* parasites. PyMiGS was detected as double bands (upper minor and lower major band) of approximately 75 kDa under non-reducing condition and as double bands of approximately 50 and 30 kDa under reducing condition (Figure 1a). The presence of multiple bands suggests that PyMiGS is subjected to post-translational cleavage. To further investigate the expression profile of PyMiGS, we performed immunofluorescence assays (IFA) using anti-PyMiGS rabbit antiserum. Punctate fluorescent signal was observed in the gametocyte cytoplasm (Figure 1b), but no signal was detected in schizonts and ookinetes (Figure 1b). These data indicate that PyMiGS is expressed in gametocytes but not expressed following transformation to ookinetes.

Sex-specific expression of PyMiGS was confirmed by double-staining IFA using anti-α-tubulin-II antiserum (a marker for male parasites) or anti-Pys25 antiserum (a marker for female parasites) to distinguish male from female. IFA images clearly showed that all PyMiGS positive gametocytes were also positive for the male marker anti-α-tubulin-II, whereas PyMiGS negative gametocytes were positive for the female marker anti-Pys25 (Figure 1b). Furthermore, anti-PyMiGS antiserum also reacted with exflagellating male gametes (microgametes; Figure 1b). PyMiGS therefore is specifically expressed in male gametocytes and microgametes.

2.2 | PyMiGS is localised to the osmiophilic body and microgamete surface

Subcellular localisation of PyMiGS was analysed using immunoelectron microscopy (IEM) before and 10 min after in vitro activation. PyMiGS subcellular localisation was observed exclusively on the MOB in the cytoplasm of male gametocytes (Figure 2a), and no reaction was

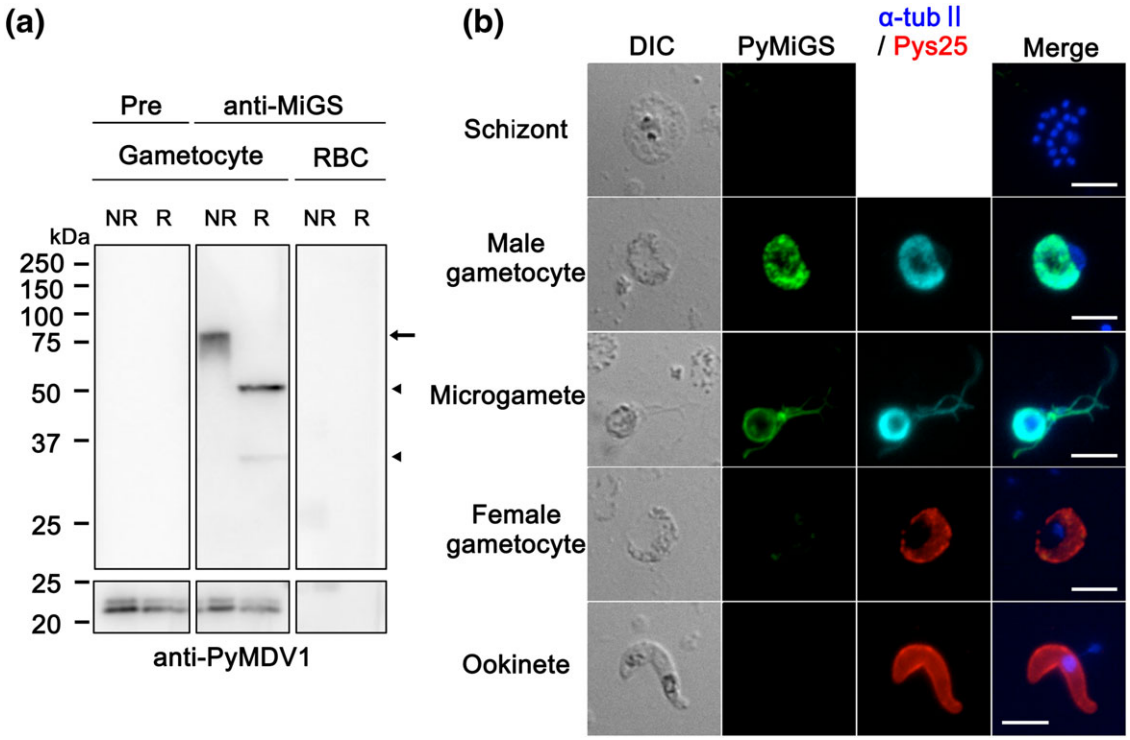

FIGURE 1 Expression and localisation of PyMiGS in *Plasmodium yoelii 17XNL*. (a) Western-blot analysis showing PyMiGS expression in gametocytes. Gametocyte enriched parasite extracts (gametocyte: 10^5 gametocytes/lane) and non-iRBC (RBC: 10^6 RBC/lane) were separated by SDS-PAGE under reducing (R) and non-reducing conditions (NR) and subjected to immunoblotting with anti-PyMiGS (anti-MiGS) antiserum at 1/5,000 dilution. Antiserum against PyMDVI/PEG3 was used as a loading control. Arrow and arrowheads indicate full-length PyMiGS (NR) and cleaved PyMiGS (R), respectively. (b) Expression of PyMiGS in asexual and sexual stage parasite revealed by immunofluorescence assay. PyMiGS (green) was specifically detected in male gametocyte and microgamete using anti-PyMiGS rabbit antiserum. Mouse anti-α-tubulin-II antibody (α-tub II cyan) was used as a male gametocyte and microgamete marker. Mouse anti-Pys25 antibody (Pys25, red) was used as a female gametocyte and ookinete marker. Nuclei were stained with DAPI (blue). Scale bars, 5 μm

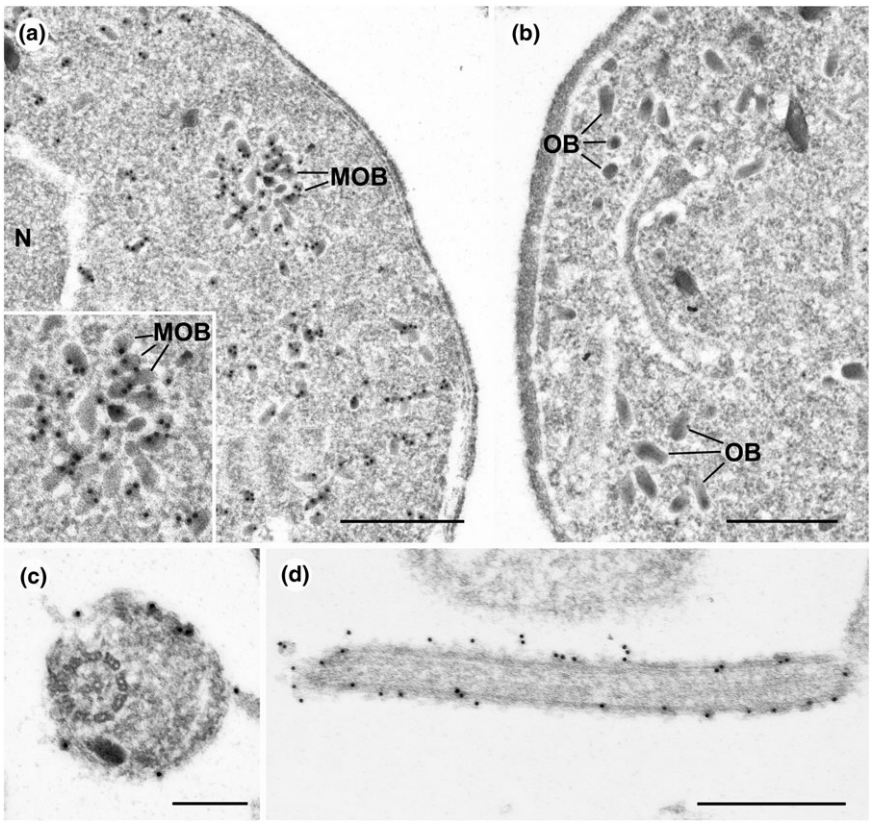

FIGURE 2 Subcellular localisation of PyMiGS in gametocytes and microgametes. (a) Male gametocyte: Immuno-gold labelling using anti-PyMiGS antiserum shows that PyMiGS is specifically localised to male osmiophilic bodies (MOB) in male gametocytes. N: nucleus. Scale bar, 500 nm. Inset: larger magnification image of MOB. (b) Female gametocyte OB, larger in size than MOB, are negative for anti-PyMiGS antiserum labelling. Scale bar, 500 nm. (c) Cross section of a microgamete showing surface labelling of PyMiGS. Scale bar, 200 nm. (d) Transverse section of a microgamete showing surface labelling of PyMiGS. Scale bar, 500 nm

observed on the OB of female gametocytes (Figure 2b). To further confirm those findings, we performed double staining IEM using rabbit anti-PyMiGS antiserum and mouse anti-Pyg377 antiserum (as a female OB marker; Olivieri et al., 2015). PyMiGS positive OB in male gametocytes were negative for Pyg377 (Figure S2a), and PyMiGS negative OB in female gametocytes were positive for Pyg377 (Figure S2b). The size of MOB with PyMiGS positive reactivity is smaller than that of female OB lacking PyMiGS reactivity. Longer axis length (mean ± *SD*) of MOB was 90 ± 16 nm (*n* = 175, from 12 ultrathin sections) and that of female OB was 142 ± 36 nm (*n* = 176, from 12 ultrathin sections). MOB remain scattered in the cytoplasm of activated male gametocytes after egress from RBC (Figure S3a). When microgametes were released, PyMiGS was observed in the MOB released outside the remnant cell and also on the surface of microgametes (Figure S3b). Finally, PyMiGS was detected on the surface of free microgametes (Figure 2c,d). Negative IEM reactivity was confirmed using preimmune serum of the rabbit immunised with rPyMiGS (Figure S3c).

2.3 | PyMiGS is important for OB formation in male gametocytes

To investigate the function of PyMiGS, we generated *PyMiGS*-disrupted parasites (ΔPyMiGS) by double homologous recombination to replace the endogenous *PyMiGS* locus, using a *Toxoplasma gondii DHFR/TS* expression cassette as a selectable marker (Figure S4a). We succeeded in generating two clones (ΔPyMiGS Cl#1 and ΔPyMiGS Cl#2) derived from independent experiments. Successful integration of the selectable marker into *PyMiGS* locus by homologous recombination was confirmed by genotyping PCR (Figure S4b). The absence of PyMiGS protein expression in male gametocytes of ΔPyMiGS clones was confirmed by western blotting (Figure S4c).

Mutant asexual stage parasites (ΔPyMiGS) proliferated at similar efficiency as wild-type parasites (PyWT) in mice, indicating that PyMiGS has no essential role in blood-stage development (Figure 4c upper panel). Blood smears from ΔPyMiGS-infected mice were double-stained using anti-α-tubulin-II (male marker) antibody and anti-Pys25 (female marker), which allowed counting of male and female gametocyte numbers. The sex ratio of the two mutant clones was comparable to that of PyWT (Figure S4d), suggesting that male gametocyte development was not impaired in ΔPyMiGS parasites.

Morphological changes of gametocytes and gametes of ΔPyMiGS were observed by transmission electron microscopy. ΔPyMiGS showed a marked decrease in the number of MOB in the cytoplasm of male gametocytes. Therefore, the number of OB in PyWT and ΔPyMiGS gametocytes were counted using IEM images stained with anti-PyMDV1/PEG3 antiserum. PyMDV1/PEG3 is known to localise to OB in both male and female gametocytes and play an important role in gametocyte egress from RBC (Olivieri et al., 2015; Ponzi et al., 2009). In ΔPyMiGS gametocytes, the number and shape of female OB labelled by anti-PyMDV1/PEG3 antiserum were similar to those of PyWT (Figures 3a,b,c and S5a,b). In contrast, the number of MOB was markedly reduced in ΔPyMiGS (10.4 ± 4.0 in 10 μm^2 cytoplasm)

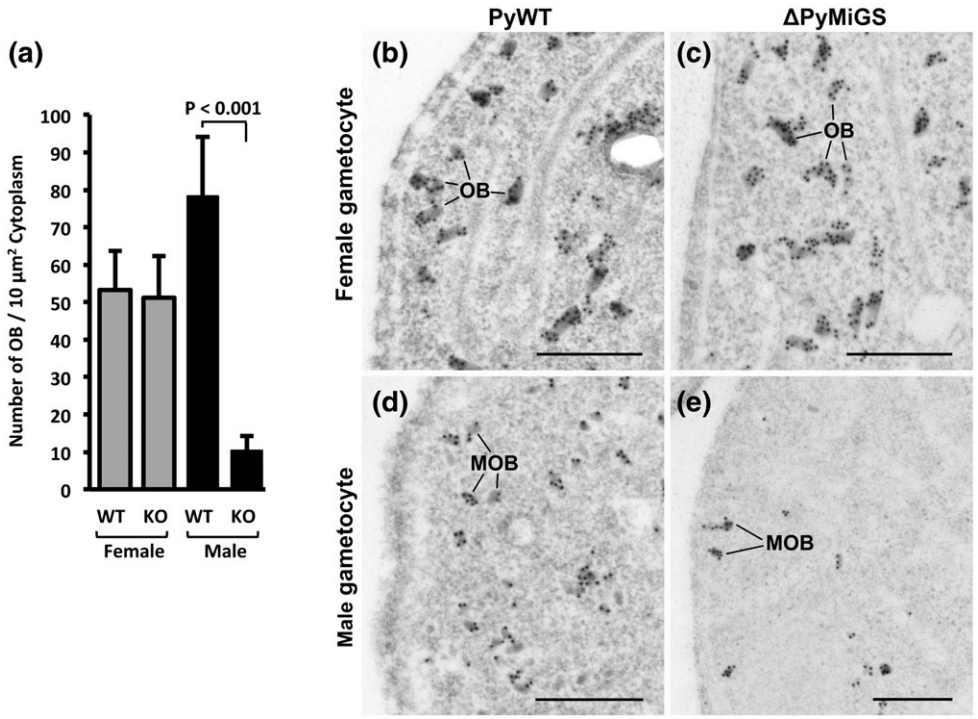

FIGURE 3 Impairment of MOB formation in ΔPyMiGS male gametocytes confirmed by IEM. (a) Number of OB counted in the cytoplasm of PyWT (WT) and ΔPyMiGS (KO) gametocytes. The number of OB per 10 μm^2 cytoplasm was calculated based on an area measured using Image J. IEM sections of PyWT female gametocyte (*n* = 25), ΔPyMiGS female gametocyte (*n* = 24), PyWT male gametocyte (*n* = 25), and ΔPyMiGS male gametocyte (*n* = 26) were used for the measurement. (b–e) Immunoelectron microscopy showing OB of PyWT and ΔPyMiGS gametocytes detected by PyMDV1/PEG3 labelling. (b) Female gametocytes of PyWT. OB labelled by anti-PyMDV1/PEG3 antiserum are scattered in the cytoplasm. Scale bar, 500 nm. (c) Female gametocytes of ΔPyMiGS. OB of labelled by anti-PyMDV1/PEG3 antiserum are scattered in the cytoplasm. Scale bar, 500 nm. (d) Male gametocytes of PyWT. MOB smaller than female OB labelled by anti-PyMDV1/PEG3 antiserum are scattered in the cytoplasm. Scale bar, 500 nm. (e) Male gametocytes of ΔPyMiGS. MOB are labelled with gold particles but the number of MOB observed in the cytoplasm are markedly reduced. Scale bar, 500 nm

compared to that of PyWT (78.3 ± 15.7 in 10 μm^2 cytoplasm), but the packaging of MDV1/PEG3 to the limited number of MOB was not influenced (Figures 3a,d,e and S5c,d). These observations strongly suggest that PyMiGS has an important role in the formation of MOB.

2.4 | PyMiGS is dispensable for gametocyte egress from the erythrocyte

Because there are several reports that molecules localised in OB are involved in gametocyte egress from RBC, we examined the egression efficiency of ΔPyMiGS gametocytes. After incubating iRBC containing gametocytes in activation medium for 15 min, the presence or absence of RBC membrane surrounding the gametocytes was examined using anti-TER-119 antibody (Olivieri et al., 2015; Figure 4a). In PyWT, 77% of male gametocytes had lost surrounding RBC membrane. Similarly, roughly 71% of ΔPyMiGS male gametocytes lost surrounding RBC membranes and successfully egressed from RBC (Figure 4b). The ratio of female gametocytes egressed from RBC was not significantly different between ΔPyMiGS and PyWT (Figure 4c). This result was further confirmed by electron microscopy showing that activated ΔPyMiGS gametocytes completely lost surrounding PVM and RBC membranes after incubation in the activation medium for 10 min

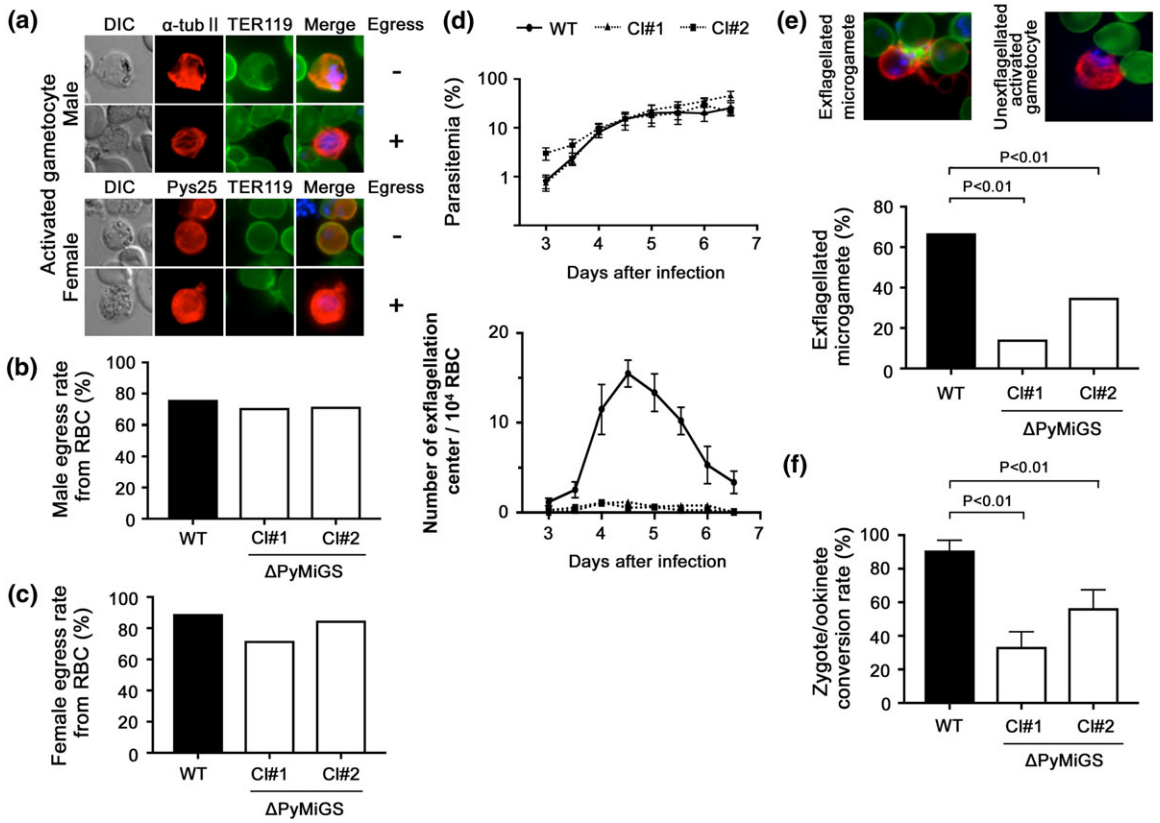

FIGURE 4 Phenotypic analysis of ΔPyMiGS during mosquito stage development. (a) Images of activated male and female gametocytes. Gametocyte egress rate was assessed 15 or 30 min after activation. Gametocytes were classified as male or female using anti-α-tubulin-II antibody (male) or anti-Pys25 antibody (female). The RBC membrane was labelled with anti-TER119 antibody. Nonegressed gametocytes indicated by TER119-positive staining are shown in the upper panels (male and female gametocytes). Egressed gametocytes indicated by TER119-negative parasite are shown in the lower panels (male and female gametocytes). (b) Male gametocyte egress efficiency from RBC. The number of male gametocytes with or without surrounding RBC membrane was counted in PyWT and ΔPyMiGS 15 min after activation. Egress rate was calculated as the number of gametocytes lacking RBC membrane divided by the total number of male gametocytes. WT: PyWT, Cl#1: ΔPyMiGS Clone #1, Cl#2: ΔPyMiGS Clone #2. (c) Female gametocyte egress efficiency from RBC. To confirm the egress of female gametocytes from RBC, the presence or absence of RBC membrane surrounding female parasites was assessed 30 min after activation. WT: PyWT, Cl#1: ΔPyMiGS Clone #1, Cl#2: ΔPyMiGS Clone #2. (d) Exflagellation centre formation was examined 5 min after activation of iRBC collected from mice at Day 3 to Day 6 postinfection. Upper panel shows the erythrocytic parasite growth of both PyWT and ΔPyMiGS. Lower panel shows the number of exflagellation centres of PyWT (solid line) and ΔPyMiGS (broken lines). The number of exflagellation centres was calculated from the number of actively moving gametes interacting with neighbouring RBC in 10,000 RBC. Each dot represents a mean value from five mice. Vertical range on each dot represents the standard error. (e) The ratio of male gametes showing exflagellation in the egressed male gametes 15 min after activation. RBC membrane was detected using anti-TER119 antibody (green), and axonemes or microgametes were detected using anti-α-tubulin-II antibody (red). Representative images of exflagellated microgamete (left) and exflagellation-suspended activated male gametocyte (right) are shown. WT: PyWT, Cl#1: ΔPyMiGS Clone #1, Cl#2: ΔPyMiGS Clone #2. Statistical analysis was performed using the Chi-square test. (f) Zygote/ookinete conversion rate was determined as the percentage of female sexual stage parasites developing into zygotes or ookinetes. Mosquito midguts were harvested 8 to 9 hr postfeeding and parasites in the midgut were identified by IFA using anti-Pys25 antibody as a marker. The zygote/ookinete conversion rate was calculated as the number of zygotes/ookinetes divided by the total number of female gametocytes, female gametes, zygotes, and ookinetes. Statistical analysis was performed using the Chi-square test

(Figure S6a). These results indicate that PyMiGS is dispensable for gametocytes to egress from RBC.

2.5 | PyMiGS plays an important role in exflagellation

To investigate whether *PyMiGS*-disruption affects the exflagellation process in vitro, the numbers of "exflagellation centres," in which flagella-like emerging microgametes adhere to and actively aggregate neighbouring RBC, was counted after 5 min incubation in the activation medium. When mouse blood was collected 4 days after infection, a remarkable impairment in the number of exflagellation centre formation was observed in ΔPyMiGS compared to PyWT (Figure 4d). The number of exflagellation centre formation of ΔPyMiGS was not increased even if the incubation time in the activation medium was extended up to 1 hr. This finding was supported by IFA observation using the parasites collected at 15 min after activation. Sixty-six percent of PyWT male activated gametocytes performed exflagellation, whereas 14% to 35% of ΔPyMiGS male activated gametocytes exflagellated (Chi-square test; $p < .01$; Figure 4e). The production of axonemes in unexflagellated ΔPyMiGS activated male gametocytes was confirmed by EM (Figure S6a). We also confirmed by EM that the condensed chromatin areas inside the nuclear envelope were formed in the activated ΔPyMiGS male gametocytes. Furthermore, a close association of axoneme with the condensed chromatin material extending from the nuclear budding (Sinden et al., 1976) was observed in the activated ΔPyMiGS male gametocytes (Figure S6a). This finding suggests that in ΔPyMiGS, activated male gametocytes mature almost normally until the late stage of microgametocyte development.

To further confirm the effects of *PyMiGS*-disruption on exflagellation in vivo, the zygote/ookinete conversion rate and transmission efficiency of ΔPyMiGS to mosquitoes was analysed in experimental infections to *Anopheles stephensi*. Conversion rates to zygote/ookinete in the mosquito midgut 8–9 hr after blood feeding were evaluated by immunostaining using anti-Pys25 antibody specifically recognising the surface of zygotes and ookinetes. In the case of PyWT, 91% of female gametocytes transformed to zygotes or further developed to ookinetes. In contrast, only 34% of ΔPyMiGS Clone #1 and 57% of ΔPyMiGS Clone #2 transformed to zygote or ookinetes. Therefore, the conversion from gamete to zygote/ookinete in the mosquito midgut was significantly reduced in ΔPyMiGS compare to PyWT (chi-square test; $p < .01$; Figure 4f). In addition, the oocyst numbers of ΔPyMiGS on Day 10 postfeeding were also decreased compared with those of PyWT (Figure S6b). This reduction was comparable to the reduction of zygote/ookinete conversion rate observed in the ΔPyMiGS gametes. In summary, these experiments demonstrated that despite the impaired MOB formation in ΔPyMiGS male gametocytes, parasite egress from erythrocyte occurred normally. In contrast, the subsequent exflagellation process was impaired in ΔPyMiGS male gametocytes, suggesting that PyMiGS has an important role in the microgamete exflagellation process.

2.6 | Antiserum against PyMiGS blocks transmission to the mosquito

Because PyMiGS is localised on the microgamete surface, we hypothesised that PyMiGS would be a target of transmission-blocking immunity. The ability of anti-PyMiGS rabbit antiserum to block parasite transmission to mosquitoes was investigated by direct feeding assays with passively immunised mice and *Anopheles* mosquitoes. Four mice were infected with *P. yoelii* expressing red fluorescent protein (RFP) through the life cycle (PyRFP) 4 days before mosquito feeding assay. Three mice were injected intravenously with anti-PyMiGS antiserum and one mouse was injected with preimmune serum (passive immunisation). Each mouse was used to feed different groups of mosquitoes before and after passive immunisation. Oocyst numbers

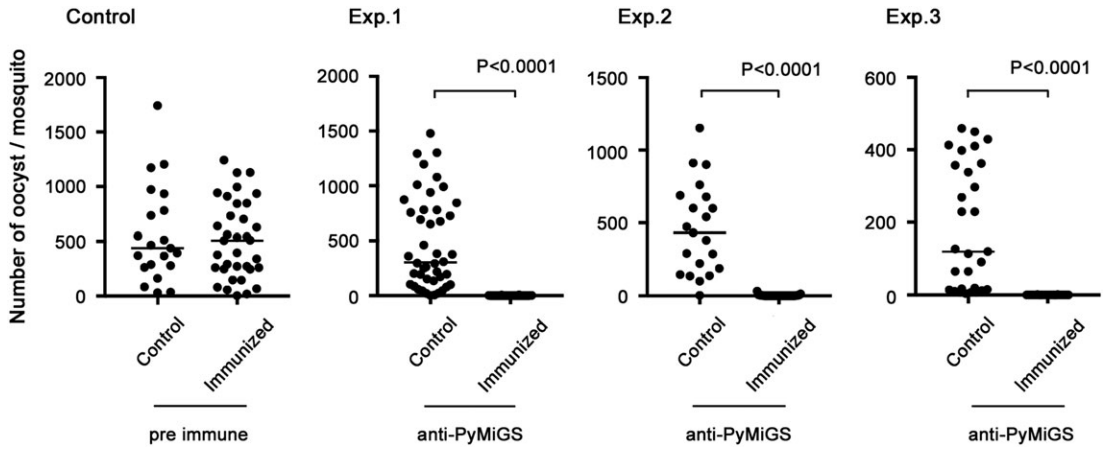

FIGURE 5 Transmission-blocking assay using anti-PyMiGS antiserum. The transmission-blocking activity of anti-PyMiGS antiserum was analysed by an in vivo passive immunisation assay. One of four mice infected with PyRFP (Jacobs-Lorena et al., 2010) was passively immunised with preimmune serum and the other three were passively immunised with anti-PyMiGS antiserum. The first group of mosquitoes (control) was fed on each mouse before passive immunisation and the second group of mosquitoes (immunised) was fed after passive immunisation. Oocyst numbers on the mosquito midgut were counted 4 days after blood feeding. Mosquito numbers used in each feeding assay are as follows: Preimmune serum, control ($n = 21$), immunised ($n = 35$); anti-PyMiGS1, control ($n = 44$), immunised ($n = 46$); anti-PyMiGS2, control ($n = 21$), immunised ($n = 31$); anti-PyMiGS3, control ($n = 29$), immunised ($n = 30$). The statistical difference in oocyst numbers between control and immunised was calculated by the Mann–Whitney U test. Passive immunisation with preimmune serum served as a negative control

formed on the mosquito midguts were counted 4 days after blood feeding. When preimmune rabbit serum was injected into an infected mouse, the median number of oocyst per midgut from the preadministration control group (control) and postadministration immunised group (immunised) were 439 and 508, respectively (p = .7341; Figure 5 control). In contrast, when anti-PyMiGS antiserum was injected, oocyst numbers from the immunised group dramatically decreased with more than 99% reduction of oocyst formation compared with those of the control group (Mann–Whitney U test; p < .0001; Figure 5, Exp. 1). Similar high transmission-blocking efficacy of anti-PyMiGS antiserum was observed in the other two blood feeding experiments (Figure 5, Exp. 2 and Exp. 3). To further confirm the transmission-blocking efficacy of anti-PyMiGS antiserum, we counted the number of sporozoites in salivary glands of mosquitoes from Exp. 3 on Day 14 after blood feeding. For "control" mosquitoes (n = 15) that had been fed before passive immunisation, 6,680 sporozoites per mosquito were collected from the salivary glands. In contrast, the number of sporozoite from the salivary glands of "immunised" mosquitoes (n = 19) was decreased to undetectable levels.

3 | DISCUSSION

While screening gametocyte/gamete surface molecules to elucidate the molecular mechanisms of fertilisation and discover novel vaccine targets, we identified PyMiGS (PY17X_1451500), a protein containing an N-terminal signal peptide and transmembrane domain at the C-terminus. It also possesses an aspartyl protease-like domain, indicating that this protein belongs to the plasmepsin family. The 3D structure prediction using Phyre2 demonstrated that PyMiGS and its orthologue in *Plasmodium falciparum* (PF3D7_1234400) shared the 3D structure resembling *Plasmodium vivax* Plasmepsin V, a protease required for cleavage of the PEXEL motif of exported proteins. In PyMiGS, one of the two active aspartic acid residues required for protease activity is replaced by a threonine residue, which strongly suggests that PyMiGS does not have protease activity. It would be interesting to elucidate its mode of action in further studies, for instance, determining if the protein regulates other acid protease family proteins during OB formation and exflagellation.

In a previous proteome analysis, it was suggested that PBANKA-1449000, an orthologue of PyMiGS, is expressed in male gametocytes (Khan et al., 2005; Talman et al., 2014). Recently, PBANKA-1449000 was identified as interacting with the known OB protein, MDV1/PEG3 (Kehrer et al., 2016). To clarify the expression profile of this molecule, we have produced a specific antibody against recombinant PyMiGS. IFA showed that PyMiGS is specifically expressed in male gametocytes by double staining with anti-PyMiGS antiserum and anti-α-tubulin-II antiserum. In IEM analysis, anti-PyMiGS antiserum specifically reacted with the MOB in the cytoplasm of gametocytes. The OB are club-shaped electron-dense vesicles and mostly distributed throughout the cytoplasm of both male and female gametocytes. MOB are reported to be slightly smaller in size and fewer in number than those of females (Olivieri et al., 2015; Sinden et al., 1976). The reactivity of anti-PyMiGS antiserum was negative in female gametocytes with relatively large OB, but the antiserum reacted specifically to male gametocytes with MOB in the cytoplasm. Based on the above results, it is concluded that PyMiGS is expressed exclusively in MOB of male gametocytes but not OB of females. Following male gametocyte activation and transformation to microgamete, PyMiGS is translocated to the surface of microgametes.

During egress from RBC, gametocytes disrupt two surrounding membranes in sequential fashion, first the inner PVM followed by the outer RBC membrane (Sologub et al., 2011; Wirth & Pradel, 2012). Among the molecules known to be important for membrane disruption, MDV1/PEG3 and GEST are localised to OB in both male and female gametocytes (Furuya et al., 2005; Lanfrancotti, Bertuccini, Silvestrini, & Alano, 2007; Ponzi et al., 2009; Silvestrini et al., 2005; Talman et al., 2011). Therefore, molecules localised in OB of gametocytes are thought to be involved in egress from RBC. Recently, PPLP2 and MTRAP were shown to localise in vesicles other than OB in the gametocyte cytoplasm and have also been found to function to rupture PVM and RBC membrane (Bargieri et al., 2016; Deligianni et al., 2013; Kehrer et al., 2016). Because PyMiGS is localised to the MOB, we observed the effects of *PyMiGS* disruption on gametocyte egress from RBC. The presence or absence of RBC membrane surrounding gametocytes was confirmed using anti-RBC membrane antibody (anti-TER-119) after in vitro activation. As a result, both male and female ΔPyMiGS gametocytes were shown to successfully egress from iRBC, similar to PyWT. This finding was confirmed by the electron microscopic observation that PVM and RBC membrane surrounding gametocytes were absent in ΔPyMiGS. These results indicate that PyMiGS is dispensable for gametocyte egress from RBC. Similar findings are reported for G377 that is specifically expressed in female OB (Alano et al., 1995; Severini et al., 1999). G377-deficient gametocytes could egress normally from RBC (Suaréz-Cortés, Silvestrini, & Alano, 2014; Suaréz-Cortés et al., 2016), or in a slightly delayed manner (Olivieri et al., 2015).

In *Plasmodium berghei*, gametocyte egress and ookinete formation efficiency of the *PBANKA_1449000* (PyMiGS orthologue) gene deletion mutant were similar to WT (Kehrer et al., 2016). In contrast, ookinete formation efficiency of ΔPyMiGS was significantly impaired (Figure 4f) and the number of MOB in male gametocytes was dramatically decreased; whereas OB in female gametocytes was not different from PyWT in both number and size. Similarly, in female gametocytes of G377-KO, a remarkable decrease in the number of OB and a reduction in size have been observed (de Koning-Ward et al., 2008; Olivieri et al., 2015). In addition, MDV1/PEG3, one of the egress related molecules, is detected in the OB-remnant structures in Pbg377-KO female gametocytes (Olivieri et al., 2015). Expression of MDV1/PEG3 was also confirmed in a few MOB observed in the cytoplasm of ΔPyMiGS male gametocytes. In summary, both male-specific PyMiGS and female-specific G377 play important roles for the formation of OB. MDV1/PEG3 is expressed on a small number of OB, formed in the cytoplasm of both ΔPyMiGS and G377-KO, and may allow these KO-parasites to escape from iRBC.

After mosquitoes have ingested iRBC, male and female gametocytes egress from RBC in the mosquito midgut and then male gametes release motile microgametes competent for fertilisation. After the egress of the male gamete from the RBC, the OB containing PyMiGS migrate to the subsurface space of the gamete. PyMiGS is released

into the extracellular space upon the subsequent release of microgametes, and PyMiGS is then observed on the surface of microgametes. Therefore, we hypothesised that PyMiGS performs a role during microgamete release. In vitro activation experiments revealed that the formation of exflagellation centres by ΔPyMiGS was markedly reduced as compared with PyWT. Electron microscopic observation revealed that closely associated flagella-like axonemes and condensed chromatin materials extending from the nuclear budding were retained in the late stage of activated ΔPyMiGS male gametocytes even after 15 min of activation. These observations suggest that PyMiGS plays a role in the release of microgametes.

Surface localisation of PyMiGS on the microgamete suggests the possibility that PyMiGS has the role in fertility, including recognition/attachment (such as P48/45) or fusion (such as HAP2/GCS1) to fertile female gametes (Hirai et al., 2008; Liu et al., 2008; van Dijk et al., 2001). Therefore, we investigated the zygote/ookinete conversion rate in the mosquito midgut at 9 hr after a blood meal and found that the conversion rate of ΔPyMiGS is almost half of that of PyWT (Figure 4f). This rate is equivalent to the proportion of male gametes in ΔPyMiGS in which release of microgametes was confirmed at 15 min after activation in vitro (Figure 4e). Therefore, the difference between PyWT and ΔPyMiGS zygote/ookinete conversion rates probably reflects the difference in the capacity for microgamete release in these parasites. In summary, ΔPyMiGS likely has a defect in the process of exflagellation and subsequent fertilisation (such as recognition and fusion to female gametes), zygote formation. The ookinete conversion rate of ΔPbMiGS is reported to be similar to that of WT (Kehrer et al., 2016), which is different from the phenotype of ΔPyMiGS shown in this study. Species differences in phenotype of OB protein have also been reported in gametocyte egress efficiency from erythrocyte between ΔPfg377 and ΔPbg377 (Olivieri et al., 2015; Suaréz-Cortés et al., 2014). To further understand the role of MiGS, it is desirable to observe the phenotypic changes in *P. falciparum* MiGS deficient parasites.

Development of a malaria TBV is considered to be an essential component (HTTP://WWW.WHO.INT/IMMUNIZATION/TOPICS/MALARIA/VACCINE_ROADMAP/TRM_UPDATE_NOV13.PDF) towards malaria elimination; however, the malaria TBV candidate molecules with potential for practical use are limited to date; such as P25 targeting the zygote/ookinete, P230 and P48/45 targeting the gametocyte/gamete, and HAP2/GCS1 targeting the microgamete (Miura et al., 2013; Nikolaeva, Draper, & Biswas, 2015; Tachibana et al., 2011; Theisen, Jore, & Sauerwein, 2017; Wu, Sinden, Churcher, Tsuboi, & Yusibov, 2015). Although the effectiveness of P25, a leading TBV antigen, is widely recognised, clinical trials have revealed difficulties in vaccine development due to poor immunogenicity in the human body (Wu et al., 2008). Therefore, there is now an urgent need to find novel target molecules, along with the improvement of antigen presentation methods (Jones et al., 2013; Qian et al., 2007; Wu et al., 2006). Based on the results that PyMiGS translocates to the surface of microgametes after exflagellation, we hypothesised that the function of surface-exposed PyMiGS could be disrupted by immune sera and therefore determined the transmission-blocking activity of rabbit anti-PyMiGS antibody. As shown in Figure 5, when mosquitoes were fed on Py-infected mice passively immunised with anti-PyMiGS antiserum, anti-PyMiGS antiserum demonstrated nearly 100% transmission-inhibitory efficacy. This promising result paves the way for the development of the *PyMiGS* orthologues in *P. falciparum* and *P. vivax* as components of a novel TBV.

4 | EXPERIMENTAL PROCEDURES

4.1 | Mice

ICR and BALB/C female mice, 6–8-week-old (Nippon CREA, Tokyo, Japan) at the time of primary infection, were used throughout the study. Mice were kept in a room with a temperature of 22 °C under a 12-hr-light/12-hr-dark cycle. All animal experimental protocols were approved by the Institutional Animal Care and Use Committee of Ehime University and the experiments were conducted according to the Ethical Guidelines for Animal Experiments of Ehime University.

4.2 | Parasites

Plasmodium yoelii 17XNL (PyWT) was maintained in ICR mice. The *P. yoelii* 17XNL strain expressing DsRed driven by elongation factor 1 α promoter (PyRFP; Jacobs-Lorena, Mikolajczak, Labaied, Vaughan, & Kappe, 2010) was provided by the Center for Infectious Disease Research, Seattle, USA.

4.3 | Targeted gene disruption of *PyMiGS*

PyMiGS disrupted parasites (ΔPyMiGS) were generated by double crossover homologous recombination using the gene disruption vector pL0001 available from BEI Resources (https://www.beiresources.org/MR4Home.aspx). To replace the endogenous *PyMiGS* genomic locus with the selectable marker containing the pyrimethamine-resistant *dhfr/ts* of *Toxoplasma gondii*, we cloned the 5′ and 3′ flanking regions of *PyMiGS* upstream and downstream, respectively, of the selection cassette of pL0001. The 5′ flanking region (793 bp) and the 3′ flanking region (849 bp) of the *PyMiGS* were amplified from PyWT genomic DNA (gDNA) using PY17X_1451500-5-F1-ApaI (5′-gagagggcccACATCTTTTGGATTCTATAACTTTTTTC-3′) and PY17X_1451500-5-R1-HindIII (5′-CTCTAAGCTTGCAGTAGAAGAATTTGCAATAGTTAAA-3′), PY17X_1451500-3-F1-EcoRI (5′-gagagaattcTGTGTGCATAAATAAAACCCCATGG-3′) and PY17X_1451500-3-R1-BamHI (5′-CTCTGGATCCCATTGTTCGCTATCCGCGCACAC-3′), respectively. The fragments were inserted into ApaI and HindIII sites or EcoRI and BamHI sites, respectively. The plasmids were digested with ApaI and BamHI before transfection. Enriched schizonts of PyWT were transfected with 20 μg of digested plasmid by electroporation using Nucleofector (Lonza Japan Ltd. Tokyo, Japan) with a human T cell solution and the U-33 programme and then parasites were selected with pyrimethamine (Janse, Ramesar, & Waters, 2006). The integration of the target DNA fragment was determined by PCR, using PY17X_1451500 5UTR tg-F1 (5′-GAAAGAAATATAGCGATAACATTGACG-3′) and pL0001 5pbdhfr/tsR2 (5′-AAATTTAAAAAAATAAAAGGGAAATCAATG-3′). Wild type were detected by PCR using PY17X_1451500 5UTR tg-F1 and PY17X_1451500-WT-R1 (5′-TAATGTTTCTGTATCTGGAGA

GGG-3′). ΔPyMiGS were cloned by limiting dilution. Clone #1 (Cl#1) and Clone #2 (Cl#2) were obtained following independent transfections.

4.4 | Parasite preparation

ICR mice, pretreated with 200 µl of 6 mg/ml phenyl-hydrazine (Wako Pure Chemical, Japan) in 1× PBS 3 days before, were intraperitoneally injected with PyWT or ΔPyMiGS infected blood. Infected blood (around 5% parasitemia) was collected by cardiac puncture at Day 4 after infection. Gametocyte-rich fractions containing schizonts were collected by NycoPrep™ 1.077 (Progen Biotechnik, Heidelberg, Germany). For in vitro ookinete culture, iRBC were washed with incomplete RPMI1640 medium and resuspended in ookinete culture medium (RPMI1640 containing 25 mM HEPES, 20% fetal calf serum, 24 mM sodium bicarbonate, 100 µM xanthurenic acid, 50 mg/L hypoxanthine, and pH 7.6) and incubated at 24 °C for 16 hr. Ookinete-rich fractions containing schizonts were collected by NycoPrep™ 1.077.

4.5 | Recombinant proteins and antisera production

A fragment encoding PyMiGS without the N-terminal signal peptide and C-terminal transmembrane region (amino acid positions [aa] 25–573) was amplified by PCR, using primer pairs PY17X_1451500-Xho-F1 (5′-gagactcgagTCCGTACAATCTCACAGCAATTTG-3′) and PY17X_1451500-BamH-R2 (5′-gagaggatcctcaGGCTGTTTTATTTTTTTCGTAAAAACC-3′).

A fragment encoding PyMDV1/PEG3 without an N-terminal signal peptide (amino acid positions [aa] 26–229) was amplified from PyWT cDNA by PCR, using primer pairs PY17X_1434500-Xho-F1 (5′-gagactcgagTACGAATGCATGAATATAAAAGGTTCA-3′) and PY17X_1434500-BamH-R1 (5′-gagaggatccttaATGATGTGGGTTTATGTCCTTTTC-3′).

A fragment encoding C-terminal of α-tubulin-II (amino acid positions [aa] 156–451) was amplified from *P. falciparum* NF54 gDNA by PCR, using primer pairs α-tublin-II_XhoI_F2 (5′-gagactcgagAGGTTGGCAATAGATTATGGAAAG-3′) and α-tublin-II BamHI_R2 (5′-gagaggatcctcaTTCATATCCCTCATCTTCTCC-3′).

A fragment encoding Pyg377 (amino acid positions [aa] 2004–2204) was amplified from PyWT blood stage cDNA by PCR, using primer pairs PY17X_1465600-Xho-F1 (5′-gagactcgagAAATTAATAGAACCATTTGTACCTATTAG-3′) and PY17X_1465600-BamH-R1 (5′-gagaggatcctcaTTCTTTATTTCCTGTTTTATTTAATTTAT-3′).

A fragment encoding Pys25 (amino acid positions [aa] 24–193) was amplified from PyWT ookinete cDNA by PCR, using primer pairs Pys25 CF std F (5′-gagagagactcgag*ATG*GCAATTACACCAGCAACTCAATGTA-3′) and Pys25 CF std R, (5′-gagagagaggatcc*CTA*GTGATGATGATGATGGATACATTTTTCTTCTTCAACGCTAAG-3′).

The amplified PyMiGS DNA fragment was inserted between the XhoI and BamHI sites of plasmid pEU-E01-GST-TEV-N2 (CellFree Sciences). Amplified PyMDV1/PEG3, α-tublin-II Pyg377, or Pys25 DNA fragments were independently inserted between the XhoI and BamHI sites of plasmid pEU-E01-HisGST(TEV)-N2 (CellFree Sciences). DNA sequences of the inserts were confirmed using the ABI PRISM 3100 Genetic Analyzer and the BigDye Terminator v1.1 Cycle Sequencing kit (Applied Biosystems, Foster City, CA, USA). The recombinant proteins were expressed using a wheat germ cell-free system (CellFree Sciences, Matsuyama, Japan) (Tsuboi, Takeo, et al., 2008; Tsuboi, Takeo, Sawasaki, et al., 2010). After synthesis, recombinant PyMiGS was affinity purified by passage through a glutathione-Sepharose 4B column (GE Healthcare, Camarillo, CA, USA) and eluted by on-column cleavage with AcTEV protease (Invitrogen, Carlsbad, CA, USA). Expressed recombinant PyMDV1/PEG3 or Pys25 was captured by a glutathione-Sepharose 4B column and eluted with elution buffer (40 mM reduced glutathione, 50 mM Tris-HCl, 300 mM NaCl, 200 mM Imidazole, 2%glycerole, and pH 8.0). Expressed recombinant α-tubulin-II was captured by a Ni Sepharose 6 Fast Flow column (GE Healthcare, Camarillo, CA, USA) and eluted by elution buffer (20 mM sodium phosphate, 300 mM NaCl, 500 mM imidazole, and pH 8.0).

To generate antisera against PyMiGS (full-length without GST tag), PyMDV1/PEG3, α-tubulin-II, or Pys25, Japanese white rabbits were immunised subcutaneously with 250 µg of purified recombinant protein with Freund's complete adjuvant, followed by two immunisations using 250 µg of purified recombinant protein with Freund's incomplete adjuvant. All immunisations were done at 3-week intervals and antisera were collected 14 days after the last immunisation (Kitayama labes Co. Ltd. Ina, Japan). Mouse antiserum against Pys25 or Pyg377 was produced by immunising BALB/C mouse with 20 µg of recombinant protein per shot according to the protocol.

4.6 | Western blot analysis

The proteins of gametocyte-rich samples from PyWT, or ΔPyMiGS were extracted in reducing or non-reducing SDS-PAGE loading buffer, and then boiled at 97 °C for 5 min, followed by separation by electrophoresis on a 12.5% polyacrylamide gel (ATTO, Tokyo, Japan). Proteins were transferred to a 0.2 µm polyvinylidene fluoride membranes (ATTO). Membranes were incubated with Blocking One (Nacalai Tesque, Inc, Kyoto, Japan) followed by immunostaining with rabbit antisera against PyMiGS (1:5,000 dilution) as the primary antibody. Preimmune rabbit serum was used as negative control. The membranes were then probed by HRP-conjugated goat anti-rabbit IgG antibody (GE Healthcare) and visualised with Immobilon Western Chemiluminescent HRP Substrate (Millipore, Billerica, MA, USA) on a LAS 4000 mini luminescent image analyser (GE Healthcare). The relative molecular masses of the proteins were estimated with reference to Precision Plus Protein Standards (Bio-Rad, Hercules, CA, USA). PyMDV1/PEG3 or α-tubulin-II was detected using rabbit anti-PyMDV1/PEG3 antiserum (1:100 dilution) or rabbit anti-α-tubulin-II antiserum (1:100 dilution) after removal of anti-PyMiGS antibody using WB stripping solution (Nacalai tesque).

4.7 | Immunofluorescence assay

Infected blood smears were fixed on glass slides with ice-cold acetone for 5 min and blocked with PBS containing 5% non-fat milk (PBS milk) at 37 °C for 1 hr. They were then incubated with rabbit anti-PyMiGS antiserum (1:1,000 dilution) and either mouse anti-Pys25 antiserum (female gametocyte marker, 1:100 dilution) or mouse anti-α-tubulin-II antiserum (Shinzawa, Ishino, Tachibana, Tsuboi, & Torii, 2013; male

marker, 1:100 dilution) at 37 °C for 1 hr, followed by incubation with Alexa Fluor 488-conjugated goat anti-rabbit IgG and Alexa Fluor 546-conjugated goat anti-mouse IgG (Invitrogen) as a secondary antibody (1:500 dilution) at 37 °C for 30 min. Nuclei were stained with 4′,6-diamidino-2-phenylindole (DAPI; 2 μg/ml) mixed with a secondary antibody solution. Slides were mounted in ProLong Gold Antifade reagent (Invitrogen) and observed using a fluorescence microscope (Axio ScopeA1; Carl Zeiss MicroImaging, Thornwood, NY, USA).

4.8 | Electron microscopy

For IEM analysis, gametocyte- or gamete-rich infected blood was fixed for 30 min on ice in a mixture of 1% paraformaldehyde–0.2% glutaraldehyde in 1× HEPES buffer (pH 7.05). Fixed specimens were dehydrated and embedded in LR-White resin (Polysciences Inc, Warrington, PA, USA). Ultrathin sections on a grid were blocked in PBS containing 5% non-fat milk and 0.01% Tween 20 (PBS-MT) then incubated at 4 °C overnight with rabbit anti-PyMiGS antiserum (1:200 dilution) or anti-PyMDV1/PEG3 antiserum (1:100 dilution) in PBS-MT. For double staining IEM, a mixture of rabbit anti-PyMiGS antiserum (1:200 dilution) and mouse anti-Pyg377 antiserum (1:50 dilution) was used. After washing with PBS containing 0.4% BlockAce Powder (DS-Phama Co, Japan) and 0.01% Tween 20 (PBS-BT), the grids were incubated at 37 °C for 1 hr with goat anti-rabbit IgG conjugated to 15 nm gold particles (BBI International, Minneapolis, MN, USA) diluted 1:20 in PBS-MT, rinsed with PBS-BT followed by water as described (Arumugan et al., 2011). For double staining IEM, a mixture of goat anti-rabbit IgG conjugated to 5 nm gold particles and goat anti-mouse IgG conjugated to 15 nm gold particles was used as secondary antibodies. For standard TEM analysis, gametocyte- or gamete-rich infected blood were fixed for 60 min on ice in a mixture of 2% paraformaldehyde–2% glutaraldehyde in 1× HEPES buffer (pH 7.05) and further fixed in 1% osmium tetrooxide in 1× HEPES buffer for 90 min. Fixed specimens were embedded in low-melting agarose, dehydrated and then embedded in epoxy resin. Ultrathin sections were stained with uranyl acetate and lead citrate. Samples were examined with a transmission electron microscope (JEM-1230, JEOL, Japan). MOB numbers within male gametocyte and OB numbers of female gametocytes were counted using IEM images taken from PyWT or ΔPyMiGS sections labelled with anti-PyMDV1/PEG3 antiserum. The area of the cytoplasmic region in which the number of OB or MOB was measured using Image J 1.50i (NIH, USA).

4.9 | RBC egress assay

To activate gametocytes, parasite infected blood samples were mixed with ookinete culture medium and incubated at 24 °C. Samples were taken after 15 or 30 min incubation and fixed with 4% paraformaldehyde for 30 min. After washing with PBS, samples were spotted on glass slides and permeabilised with acetone. Samples were labelled with rabbit anti-Pys25 antiserum (female marker, 1:1,000 dilution) or rabbit anti-α-tubulin-II antiserum (male marker, 1:500 dilution), followed by incubation with goat anti-rabbit antibody conjugated to Alexa Fluor 546 (1:500 dilution), and then RBC membranes were labelled with rat anti-TER119 antibody conjugated to Alexa Fluor 488 (1:500 dilution, BioLegend, San Diego, USA; Olivieri et al., 2015). Cell nuclei were labelled with DAPI. Numbers of egressed or nonegressed parasites were counted using a fluorescence microscope.

4.10 | Exflagellation assay

To activate male gametocytes, 3 μl of PyWT or ΔPyMiGS infected blood were mixed with 57 μl of ookinete culture medium and incubated for 5 min at 24 °C. After incubation, samples were loaded on a hemocytometer and analysed by light microscopy to count the number of exflagellation centres per 1×10^4 RBC (Blagborough & Sinden, 2009).

4.11 | Zygote/ookinete conversion assay and oocyst count

Anopheles stephensi (SDA 500) mosquitoes were fed on ICR mice infected with PyWT or ΔPyMiGS. Fully engorged mosquitoes were collected and maintained at 24 °C with a 12-hr-light/12-hr-dark cycle. Fully engorged mosquito midguts were placed into 50 μl of PBS and disrupted to make a dilute suspension of the blood meal at 8–9 hr postblood feeding (N = 10) (Vaughan, Hensley, & Beier, 1994). Each suspension was spotted on a glass slide and fixed by cold-acetone. Female gametocytes, zygotes, and ookinetes were detected by IFA using anti-Pys25 monoclonal antibody #14 (Tsuboi, Cao, et al., 1997) as a marker. Zygote/ookinete conversion rates were assessed as the percentage of female gametocytes developed to zygotes or ookinetes. Mosquito dissections for oocyst counts were done 10 days postfeeding and the number of oocysts per mosquito midgut was counted under a microscope (Tomas et al., 2001).

4.12 | Transmission-blocking assay (direct feeding)

Four groups of *A. stephensi* mosquitoes were fed on four BALB/C mice infected with PyRFP on Day 4 postinfection as preimmunisation control groups (Figure 5 control). Each mouse was then intravenously injected with 0.2 ml of anti-PyMiGS antiserum or 0.2 ml of preimmune serum, respectively. Another four groups of mosquitoes were fed on each mouse at 10 min after passive immunisation as postpassive immunisation groups (Figure 5 immunised). Fully engorged mosquitoes were collected and maintained at 24 °C under 12-hr-light/12-hr-dark cycle. Mosquitoes were dissected on Day 4 postblood-feeding, and oocyst numbers on the midguts were counted under a fluorescence microscope. Transmission-blocking efficacy was evaluated by comparing the oocyst numbers between control and immunised groups by statistical analysis using the Mann–Whitney U test.

ACKNOWLEDGMENTS

We thank Moe Sudo for technical support with IFA and western blotting analysis. We thank Sono Sadaoka and Aki Konishi for technical support with mice and mosquito rearing. We also thank Masachika Shudo (Advanced Research Support Center, Ehime University) for technical assistance with electron microscopy. We would like to thank Dr. Stefan Kappe (Center for Infectious Disease Research, Seattle, USA) for providing parasites, Dr. Justine Boddey (Walter and Eliza Hall

Institute of Medical Research, Australia) and Dr. Yasuteru Shigeta (University of Tsukuba, Center for Computational Sciences) for valuable discussion, and Dr. Thomas Templeton (NEKKEN, Nagasaki, Japan) for critical reading of the manuscript. Plasmid pL0001 was obtained through BEI Resources, NIAID, NIH, for transfection in *Plasmodium yoelii*, MRA-770, contributed by Dr. Andrew P. Waters. This work was supported by JSPS KAKENHI Grants JP24590506, JP15K08443, and JP25670202.

CONFLICT OF INTEREST

The authors have no conflict of interest.

ORCID

Tomoko Ishino http://orcid.org/0000-0003-2466-711X

REFERENCES

Alano, P., Read, D., Bruce, M., Aikawa, M., Kaido, T., Tegoshi, T., … Elliott, J. F. (1995). COS cell expression cloning of Pfg377, a *Plasmodium falciparum* gametocyte antigen associated with osmiophilic bodies. *Molecular and Biochemical Parasitology*, *74*(2), 143–156. https://doi.org/10.1016/0166-6851(95)02491-3.

Arumugan, T. U., Takeo, S., Yamasaki, T., Thonkukiatkul, A., Miura, K., Otsuki, H., … Tsuboi, T. (2011). Discovery of GAMA, a *Plasmodium falciparum* merozoite micronemal protein, as a novel blood-stage vaccine candidate antigen. *Infection and Immunity*, *79*(11), 4523–4532. https://doi.org/10.1128/IAI.05412-11.

Bannister, L. H., Hopkins, J. M., Fowler, R. E., Krishna, S., & Mitchell, G. H. (2000). A brief illustrated guide to the ultrastructure of Plasmodium falciparum asexual blood stages. *Parasitology Today*, *16*(10), 427–433. https://doi.org/10.1016/S0169-4758(00)01755-5.

Bargieri, D. Y., Thiberge, S., Tay, C. L., Carey, A. F., Rantz, A., Hischen, F., … Menard, R. (2016). *Plasmodium* merozoite TRAP family protein is essential for vacuole membrane disruption and gamete egress from erythrocytes. *Cell Host & Microbe*, *20*(5), 618–630. https://doi.org/10.1016/j.chom.2016.10.015.

Billker, O., Miller, A. J., & Sinden, R. E. (2000). Determination of mosquito pH in situ by iron-selective microelectrode measurement: Implications for the regulation of malarial gametogenesis. *Parasitology*, *120*(6), 547–551. https://doi.org/10.1017/S0031182099005946.

Blagborough, A. M., & Sinden, R. E. (2009). *Plasmodium berghei* HAP2 induces strong malaria transmission-blocking immunity *in vivo* and *in vitro*. *Vaccine*, *27*(38), 5187–5194. https://doi.org/10.1016/j.vaccine.2009.06.069.

de Koning-Ward, T. F., Olivieri, A., Bertuccini, L., Hood, A., Silvestrini, F., Charvalias, K., … Ranford-Cartwright, L. C. (2008). The role of osmiophilic bodies and Pfg377 expression in female gametocyte emergence and mosquito infectivity in the human malaria parasite *Plasmodium falciparum*. *Molecular Microbiology*, *67*(2), 278–290. https://doi.org/10.1111/j.1365-2958.2007.06039.x.

Deligianni, E., Morgan, R. N., Bertuccini, L., Wirth, C. C., Silmon de Monerri, N. C., Spanos, L., … Siden-Kiamos, I. (2013). A perforin-like protein mediates disruption of the erythrocyte membrane during egress of *Plasmodium berghei* male gametocytes. *Cellular Microbiology*, *15*(8), 1438–1455. https://doi.org/10.1111/cmi.12131.

Furuya, T., Mu, J., Hayton, K., Liu, A., Duan, J., Nkrumah, L., … Su, X. (2005). Disruption of a *Plasmodium falciparum* gene linked to male sexual development causes early arrest in gametocytogenesis. *Proceedings of the National Academy of Sciences of the United States of America*, *102*(46), 16813–16818. https://doi.org/10.1073/pnas.0501858102.

Hirai, M., Arai, M., Mori, T., Miyagishima, S. Y., Kawai, S., Kita, K., … Matsuoka, H. (2008). Male fertility of malaria parasites is determined by GCS1, a plant-type reproduction factor. *Current Biology*, *18*(8), 607–613. https://doi.org/10.1016/j.cub.2008.03.045.

Jacobs-Lorena, V. Y., Mikolajczak, S. A., Labaied, M., Vaughan, A. M., & Kappe, S. H. (2010). A dispensable Plasmodium locus for stable transgene expression. *Molecular and Biochemical Parasitology*, *171*(1), 40–44. https://doi.org/10.1016/j.molbiopara.2009.12.009.

Janse, C. J., Ramesar, J., & Waters, A. P. (2006). High-efficiency transfection and drug selection of genetically transformed blood stages of the rodent malaria parasite Plasmdoium berghei. *Nature Protocols*, *1*(1), 346–356. https://doi.org/10.1038/nprot.2006.53.

Jones, R. M., Chichester, J. A., Mett, V., Jaje, J., Tottey, S., Manceva, S., … Yusibov, V. (2013). A plant-produced Pfs25 VLP malaria vaccine candidate induces persistent transmission blocking antibodies against *Plasmodium falciparum* in immunized mice. *PLoS One*, *8*(11), e79538. https://doi.org/10.1371/journal.pone.0079538.

Kehrer, J., Frischknecht, F., & Mair, G. R. (2016). Proteomic analysis of the *Plasmodium berghei* gametocyte egressome and vesicular bioID of osmiophilic body proteins identifies merozoite TRAP-like protein (MTRAP) as an essential factor for parasite transmission. *Molecular & Cellular Proteomics*, *15*, 2852–2862. https://doi.org/10.1074/mcp.M116.058263.

Khan, S. M., Franke-Fayard, B., Mair, G. R., Lasonder, E., Janse, C. J., Mann, M., & Waters, A. P. (2005). Proteome analysis of separated male and female gametocytes reveals novel sex-specific *Plasmodium* biology. *Cell*, *121*(5), 675–687. https://doi.org/10.1016/j.cell.2005.03.027.

Lanfrancotti, A., Bertuccini, L., Silvestrini, F., & Alano, P. (2007). *Plasmodium falciparum*: mRNA co-expression and protein co-localization of two gene products upregulated in early gametocytes. *Experimental Parasitology*, *116*(4), 497–503. https://doi.org/10.1016/j.exppara.2007.01.021.

Liu, Y., Tewari, R., Ning, J., Blagborough, A. M., Garbom, S., Pei, J., … Billker, O. (2008). The conserved plant sterility gene HAP2 functions after attachment of fusogenic membranes in *Chlamydomonas* and *Plasmodium* gametes. *Genes & Development*, *22*(8), 1051–1068. https://doi.org/10.1101/gad.1656508.

Miura, K., Takashima, E., Deng, B., Tullo, G., Diouf, A., Moretz, S. E., … Tsuboi, T. (2013). Functional comparison of *Plasmodium falciparum* transmission-blocking vaccine candidates by the standard membrane-feeding assay. *Infection and Immunity*, *81*(12), 4377–4382. https://doi.org/10.1128/IAI.01056-13.

Nikolaeva, D., Draper, S. J., & Biswas, S. (2015). Toward the development of effective transmission-blocking vaccines for malaria. *Expert Review of Vaccines*, *14*(5), 653–680. https://doi.org/10.1586/14760584.2015.993383.

Olivieri, A., Bertuccini, L., Deligianni, E., Franke-Fayard, B., Curra, C., Siden-Kiamos, I., … Ponzi, M. (2015). Distinct properties of the egressrelated osmiophilic bodies in male and female gametocytes of the rodent malaria parasite *Plasmodium berghei*. *Cellular Microbiolology*, *17*(3), 355–368. https://doi.org/10.1111/cmi.12370.

Ponzi, M., Siden-Kiamos, I., Bertuccini, L., Curra, C., Kroeze, H., Camarda, G., … Alano, P. (2009). Egress of *Plasmodium berghei* gametes from their host erythrocyte is mediated by the MDV-1/PEG3 protein. *Cellular Microbiology*, *11*(8), 1272–1288. https://doi.org/10.1111/j.1462-5822.2009.01331.x.

Qian, F., Wu, Y., Muratova, O., Zhou, H., Dobrescu, G., Duggan, P., … Mullen, G. E. (2007). Conjugating recombinant proteins to *Pseudomonas aeruginosa* ExoProtein A: A strategy for enhancing immunogenicity of malaria vaccine candidates. *Vaccine*, *25*(20), 3923–3933. https://doi.org/10.1016/j.vaccine.2007.02.073.

Severini, C., Silvestrini, F., Sannella, A., Barca, S., Gradoni, L., & Alano, P. (1999). The production of the osmiophilic body protein Pfg377 is associated with stage of maturation and sex in *Plasmodium falciparum* gametocytes. *Molecular and Biochemical Parasitology*, *100*(2), 247–252. https://doi.org/10.1016/S0166-6851(99)00050-X.

Shinzawa, N., Ishino, T., Tachibana, M., Tsuboi, T., & Torii, M. (2013). Phenotypic dissection of a Plasmodium-refractory strain of malaria vector Anopheles stephensi: The reduced susceptibility to P. berghei and P. yoelii. *PLoS One*, *23*;8(5), e63753. https://doi.org/10.1371/journal.pone.0063753.

Silvestrini, F., Bozdech, Z., Lanfrancotti, A., Di Giulio, E., Bultrini, E., Picci, L., … Alano, P. (2005). Genome-wide identification of genes upregulated at the onset of gametocytogenesis in *Plasmodium falciparum*. *Molecular and Biochemical Parasitology*, *143*(1), 100–110. https://doi.org/10.1016/j.molbiopara.2005.04.015.

Sinden, R. E. (1984). The biology of *Plasmodium* in the mosquito. *Experientia*, *40*(12), 1330–1343. https://doi.org/10.1007/BF01951886.

Sinden, R. E., Canning, E. U., & Spain, B. (1976). Gametogenesis and fertilization in *Plasmodium yoelii nigeriensis*: A transmission electron microscopic study. *Proceedings of the Royal Society B: Biological Sciences*, *193*(1110), 55–76. https://doi.org/10.1098/rspb.1976.0031.

Sologub, L., Kuehn, A., Kern, S., Przyborski, J., Schillig, R., & Pradel, G. (2011). Malaria proteases mediate inside-out egress of gametocytes from red blood cells following parasite transmission to the mosquito. *Cellular Microbiology*, *13*(6), 897–912. https://doi.org/10.1111/j.1462-5822.2011.01588.x.

Suaréz-Cortés, P., Sharma, V., Bertuccini, L., Costa, G., Bannerman, N. L., Sannalla, A. R., … Alano, P. (2016). Comparative proteomics and functional analysis reveal a role of *Plasmodium falciparum* osmiophilic bodies in malaria parasite transmission. *Molecular & Cellular Proteomics*, *15*(10), 3243–3255. https://doi.org/10.1074/mcp.M116.060681.

Suaréz-Cortés, P., Silvestrini, F., & Alano, P. (2014). A fast, non-invasive, quantitative staining protocol provides insights in *Plasmodium falciparum* gamete egress and in the role of osmiophilic bodies. *Malaria Journal*, *13*, 389. https://doi.org/10.1186/1475-2875-13-389.

Tachibana, M., Wu, Y., Iriko, H., Muratova, O., MacDonald, N. J., Sattabongkot, J., … Tsuboi, T. (2011). N-terminal prodomain of Pfs230 synthesized using a cell-free system is sufficient to induce complement-dependent malaria transmission-blocking activity. *Clinical and Vaccine Immunology*, *18*(8), 1343–1350. https://doi.org/10.1128/CVI.05104-11.

Talman, A. M., Lacroix, C., Marques, S. R., Blagborough, A. M., Carzaniga, R., Menard, R., & Sinden, R. E. (2011). PbGEST mediates malaria transmission to both mosquito and vertebrate host. *Molecular Microbiology*, *82*(2), 462–474. https://doi.org/10.1111/j.1365-2958.2011.07823.x.

Talman, A. M., Prieto, J. H., Marques, S., Ubaida-Mohien, C., Lawniczak, M., Wass, M. N., … Sinden, R. E. (2014). Proteomic analysis of the *Plasmodium* male gamete reveals the key role for glycolysis in flagellar motility. *Malaria Journal*, *13*, 315. https://doi.org/10.1186/1475-2875-13-315.

Theisen, M., Jore, M. M., & Sauerwein, R. (2017). Towards clinical development of a Pfs48/45-based transmission blocking malaria vaccine. *Expert Review of Vaccines*, *16*(4), 329–336. https://doi.org/10.1080/14760584.2017.1276833.

Tomas, A. M., Margos, G., Dimopoulos, G., van Lin, L. H., De Koning-Ward, T. F., Sinha, R., … Sinden, R. E. (2001). P25 and P28 proteins of the malaria ookinete surface have multiple and partially redundant functions. *The EMBO Journal*, 1, *20*(15), 3975–3983. https://doi.org/10.1093/emboj/20.15.3975.

Tsuboi, T., Cao, Y. M., Hitsumono, Y., Yanagi, T., Kanbara, H., & Torii, M. (1997). Two antigens on zygotes and ookinetes of Plasmodium Yoelii and Plasmodium berghei that are distinct targets of transmission-blocking immunity. *Infection and Immunity*, *65*(6), 2260–2264.

Tsuboi, T., Takeo, S., Iriko, H., Jin, L., Tsuchimochi, M., Matsuda, S., … Endo, Y. (2008). Wheat germ cell-free system-based production of malaria proteins for discovery of novel vaccine candidates. *Infection and Immunity*, *76*, 1702–1708. https://doi.org/10.1128/IAI.01539.07.

Tsuboi, T., Takeo, S., Sawasaki, T., Torii, M., & Endo, Y. (2010). An efficient approach to the production of vaccines against the malaria parasite. *Methods in Molecular Biology*, *607*, 73–83. https://doi.org/10.1007/978-1-60327-331-2_8.

van Dijk, M. R., Janse, C. J., Thompson, J., Waters, A. P., Braks, J. A., Dodemont, H. J., … Eling, W. (2001). A central role for P48/45 in malaria parasite male gamete fertility. *Cell*, *104*(1), 153–164. https://doi.org/10.1016/S0092-8674(01)00199-4.

Vaughan, J. A., Hensley, L., & Beier, J. C. (1994). Sprogonic development of *Plasmodium yoelii* in five Anopheline species. *The Journal of Parasitology*, *80*(5), 674–681. https://doi.org/10.2307/3283245.

Wirth, C. C., Glushakova, S., Scheuermayer, M., Repnik, U., Garg, S., Schaack, D., … Pradel, G. (2014). Perforin-like protein PPLP2 permeabilizes the red blood cell membrane during egress of *Plasmodium falciparum* gametocytes. *Cellular Microbiology*, *16*(5), 709–733. https://doi.org/10.1111/cmi.12288.

Wirth, C. C., & Pradel, G. (2012). Molecular mechanisms of host cell egress by malaria parasites. *International Journal of Medical Microbiology*, *302*(4–5), 172–178. https://doi.org/10.1016/j.ijmm.2012.07.003.

World malaria report 2016. (2016). World health organization.

Wu, Y., Ellis, R. D., Shaffer, D., Fontes, E., Malkin, E. M., Mahanty, S., … Durbin, A. P. (2008). Phase 1 trial of malaria transmission blocking vaccine candidates Pfs25 and Pvs25 formulated with montanide ISA 51. *PLoS One*, *3*(7), e2636. https://doi.org/10.1371/journal.pone.0002636.

Wu, Y., Przysiecki, C., Flanagan, E., Bello-Irizarry, S. N., Ionescu, R., Muratova, O., … Miller, L. H. (2006). Sustained high-titer antibody responses induced by conjugating a malarial vaccine candidate to outer-membrane protein complex. *Proceedings of the National Academy of Sciences of the United States of America*, *103*(48), 18243–18248. https://doi.org/10.1073/pnas.0608545103.

Wu, Y., Sinden, R. E., Churcher, T. S., Tsuboi, T., & Yusibov, V. (2015). Development of malaria transmission-blocking vaccines: From concept to product. *Advances in Parasitology*, *89*, 109–152. https://doi.org/10.1016/bs.apar.2015.04.001.

SUPPORTING INFORMATION

Additional Supporting Information may be found online in the supporting information tab for this article.

How to cite this article: Tachibana M, Ishino T, Takashima E, Tsuboi T, Torii M. A male gametocyte osmiophilic body and microgamete surface protein of the rodent malaria parasite *Plasmodium yoelii* (PyMiGS) plays a critical role in male osmiophilic body formation and exflagellation. *Cellular Microbiology*. 2018;20:e12821. https://doi.org/10.1111/cmi.12821